

Possible $\Sigma(\frac{1}{2}^-)$ under the $\Sigma^*(1385)$ peak in $K\Sigma^*$ photoproduction

Puze Gao, Jia-Jun Wu and B.S. Zou

*Institute of High Energy Physics, CAS, P.O. Box 918(4), Beijing 100049, China and
Theoretical Physics Center for Science Facilities, CAS, Beijing 100049, China*

The LEPS collaboration has recently reported a measurement of the reaction $\gamma n \rightarrow K^+\Sigma^{*-}(1385)$ with linearly polarized photon beam at resonance region. The observed beam asymmetry is sizably negative at $E_\gamma = 1.8 - 2.4\text{GeV}$, in contrast to the presented theoretical prediction. In this paper, we calculate this process in the framework of the effective Lagrangian approach. By including a newly proposed $\Sigma(J^P = \frac{1}{2}^-)$ state with mass around 1380 MeV, the experimental data for both γn and γp experiments can be well reproduced. It is found that the $\Sigma(\frac{1}{2}^-)$ and/or the contact term may play important role and deserve further investigation.

PACS numbers: 14.20.Jn, 25.20.Lj, 13.60.Le, 13.60.Rj

I. INTRODUCTION

With the development of accelerator facilities, strangeness production from photon-nucleon scattering has been extensively studied at resonance region [1–9]. These experiments can provide not only more information on the properties and interactions of the known resonances, but also clues for the existence of some new resonances. For $K\Sigma^*(1385)$ photoproduction, high statistic data have been available only recently. The CLAS collaboration has studied the reaction $\gamma + p \rightarrow K^+ + \Sigma^{*0}(1385)$ with unpolarized photon beam at energy $E_\gamma = 1.5 - 4\text{ GeV}$ [2]. The LEPS collaboration has reported the reaction $\gamma + n \rightarrow K^+ + \Sigma^{*-}(1385)$, with a linearly polarized photon beam at $E_\gamma = 1.5 - 2.4\text{ GeV}$ [9]. The high statistic data and the polarized observables provide more information and challenges for theoretical studies.

Theoretical investigations on $K\Sigma^*(1385)$ photoproduction include the work by Lutz and Soyeur [10], which mainly studies the t-channel processes, the work by Döring, Oset and Strottman [11], where the role of $\Delta(1700)$ is addressed, and the work by Oh, Ko, and Nakayama [12], where the roles of N and Δ resonances in s-channel are stressed and compared with the CLAS data [2].

For the approach by Oh, Ko, and Nakayama [12], the total cross section for $\gamma + p \rightarrow K^+ + \Sigma^{*0}(1385)$ is calculated in the framework of gauge-invariant effective Lagrangians. The results are in reasonable agreement with the CLAS data [2], showing that the s-channel N and Δ resonances above $K\Sigma^*$ threshold may give important contributions to cross sections. Although this theory can well describe the total cross section of $K\Sigma^*$ photoproduction from CLAS as well as from LEPS experiment [9], the theoretical prediction deviates greatly from the data for linear beam asymmetry measured by LEPS with polarized photon beam. This is an urgent problem for theoretical studies.

From studies of baryon spectroscopy and structures, five quark $qqqq\bar{q}$ components are proposed to play important roles in some baryons [13, 14]. A few years ago, Jaffe and Wilczek have promoted a diquark-diquark-

antiquark picture for the pentaquark baryons [15]. Zhang *et al.* then studied the $J^P = \frac{1}{2}^-$ pentaquark baryons based on this picture and predicted a $\Sigma(\frac{1}{2}^-)$ state with mass around 1360 MeV [16]. A more general pentaquark model [13] without introducing explicitly diquark clusters predicts that $\Sigma(\frac{1}{2}^-)$ has a mass similar to $\Lambda(\frac{1}{2}^-)$, which is around 1405 MeV. From these two models, one would expect a $\Sigma(\frac{1}{2}^-)$ state with mass around 1380 MeV. Recent studies on $K^-p \rightarrow \Lambda\pi^+\pi^-$ process have shown some evidence for the existence of the $\Sigma(\frac{1}{2}^-)$ near 1380 MeV [17]. In this work, we study the $K\Sigma^*(1385)$ photoproduction processes with the consideration of the case that a portion of $K\Sigma(\frac{1}{2}^-)$ photoproduction is mixed in.

This paper is organized as follows. In section II, the theoretical framework is presented for the $K\Sigma^*$ and $K\Sigma(\frac{1}{2}^-)$ photoproduction from the nucleons. In section III, the numerical results for cross sections and the beam asymmetry are presented and compared with the experimental data, with some discussions. In section IV, we give the summary of this work.

II. THEORETICAL FRAMEWORK

The effective Lagrangian method is an important theoretical approach in describing the various processes at resonance region. We use the effective Lagrangians of Ref. [12] for $K\Sigma^*$ photoproduction, where the contact term is derived from Ref. [18] to keep the amplitude gauge invariant. In the following equations we use Σ^* and Σ denoting the $\Sigma^*(\frac{3}{2}^+)$ at 1385 MeV and the $\Sigma(\frac{1}{2}^-)$ near 1380 MeV, respectively.

A. $K\Sigma^*(\frac{3}{2}^+)$ photoproduction

For the reaction $\gamma N \rightarrow K\Sigma^*(\frac{3}{2}^+)$, the Feynman diagrams are shown in Fig. 1, where the incoming momenta are k and p for photon and nucleon, respectively, and the outgoing momenta are q and p' for K meson and the

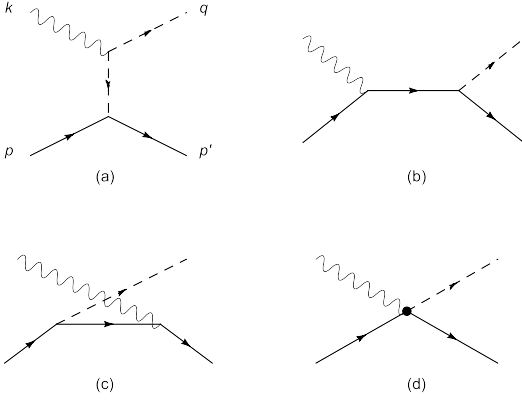


FIG. 1: Feynman diagrams for $\gamma + N \rightarrow K + \Sigma^*(\frac{3}{2}^+)$. (a) t-channel; (b) s-channel; (c) u-channel; (d) contact term.

Σ^* , respectively. From the investigation of Ref. [12], the main contributions come from the t-channel K meson exchange, the s-channel N and Δ as well as their resonances exchange, the u-channel Λ (for neutral propagator only) and $\Sigma^*(\frac{3}{2}^+)$ exchange and the contact term.

For the t-channel K meson exchange, the relevant effective Lagrangians are

$$\mathcal{L}_{\gamma KK} = ieA_\mu(K^- \partial^\mu K^+ - \partial^\mu K^- K^+), \quad (1)$$

$$\mathcal{L}_{KN\Sigma^*} = \frac{f_{KN\Sigma^*}}{m_K} \partial_\mu \bar{K} \Sigma^{*\mu} \cdot \tau N + H.c., \quad (2)$$

with the isospin structure of $K\Sigma^*N$ coupling

$$\bar{K} = (K^-, \bar{K}^0), \bar{\Sigma} \cdot \tau = \begin{pmatrix} \bar{\Sigma}^0 & \sqrt{2}\bar{\Sigma}^+ \\ \sqrt{2}\bar{\Sigma}^- & -\bar{\Sigma}^0 \end{pmatrix}, N = \begin{pmatrix} p \\ n \end{pmatrix}, \quad (3)$$

where $f_{KN\Sigma^*}$ is the coupling constant and is taken as $f_{KN\Sigma^*} = -3.22$ from the SU(3) flavor symmetry relation as in Ref. [12]; m_K is the mass for K meson.

For the s-channel nucleon exchange, the effective Lagrangians for the interactions contain Eq. (2) as well as

$$\mathcal{L}_{\gamma NN} = -e\bar{N}(\gamma^\mu A_\mu Q_N - \frac{\kappa_N}{2M_N} \sigma^{\mu\nu} \partial_\nu A_\mu)N, \quad (4)$$

where Q_N is the electric charge (in unite of e), and κ_N denotes the magnetic moment of the nucleon.

For the s-channel spin- $\frac{3}{2}$ and spin- $\frac{5}{2}$ resonances exchange, the effective Lagrangians for the interactions are

$$\mathcal{L}_{\gamma NR}(\frac{3^\pm}{2}) = -\frac{ief_1}{2M_N} \bar{N} \Gamma_\nu^{(\pm)} F^{\mu\nu} R_\mu - \frac{ef_2}{(2M_N)^2} \partial_\nu \bar{N} \Gamma^{(\pm)} F^{\mu\nu} R_\mu + H.c., \quad (5)$$

$$\mathcal{L}_{\gamma NR}(\frac{5^\pm}{2}) = \frac{ef_1}{(2M_N)^2} \bar{N} \Gamma_\nu^{(\mp)} \partial^\alpha F^{\mu\nu} R_{\mu\alpha} - \frac{ief_2}{(2M_N)^3} \partial_\nu \bar{N} \Gamma^{(\mp)} \partial^\alpha F^{\mu\nu} R_{\mu\alpha} + H.c. \quad (6)$$

and

$$\mathcal{L}_{RK\Sigma^*}(\frac{3^\pm}{2}) = -\frac{h_1}{m_K} \partial^\alpha K \bar{\Sigma}^{*\mu} \Gamma_\alpha^{(\pm)} R_\mu + \frac{ih_2}{(m_K)^2} \partial^\mu \partial^\alpha K \bar{\Sigma}_\alpha^{*\mu} \Gamma^{(\pm)} R_\mu + H.c., \quad (7)$$

$$\mathcal{L}_{RK\Sigma^*}(\frac{5^\pm}{2}) = \frac{ih_1}{m_K^2} \partial^\mu \partial^\beta K \bar{\Sigma}^{*\alpha} \Gamma_\mu^{(\mp)} R_{\alpha\beta} - \frac{h_2}{(m_K)^3} \partial^\mu \partial^\alpha \partial^\beta K \bar{\Sigma}_\mu^{*\alpha} \Gamma^{(\mp)} R_{\alpha\beta} + H.c. \quad (8)$$

where $F^{\mu\nu} = \partial^\mu A^\nu - \partial^\nu A^\mu$; R_μ and $R_{\mu\alpha}$ denote the spin- $\frac{3}{2}$ and spin- $\frac{5}{2}$ fields, respectively, and

$$\Gamma_\mu^{(\pm)} = \begin{pmatrix} \gamma_\mu \gamma_5 \\ \gamma_\mu \end{pmatrix}, \Gamma^{(\pm)} = \begin{pmatrix} \gamma_5 \\ 1 \end{pmatrix}. \quad (9)$$

For Δ and Δ resonances of isospin-3/2, the effective Lagrangians have the isospin structure

$$\begin{aligned} \bar{K} \bar{\Sigma}^* \cdot \mathbf{T}(\frac{1}{2}, \frac{3}{2}) \Delta &= \sqrt{3} K^- \bar{\Sigma}^{*+} \Delta^{++} - \sqrt{2} K^- \bar{\Sigma}^{*0} \Delta^+ \\ &\quad - K^- \bar{\Sigma}^{*-} \Delta^0 + \bar{K}^0 \bar{\Sigma}^{*+} \Delta^+ - \sqrt{2} \bar{K}^0 \bar{\Sigma}^{*0} \Delta^0 \\ &\quad - \sqrt{3} \bar{K}^0 \bar{\Sigma}^{*-} \Delta^- \quad (10) \end{aligned}$$

We consider 3 PDG resonances in s-channel, namely, $N_{\frac{3}{2}^-}(2080)$, $\Delta_{\frac{3}{2}^-}(1940)$ and $\Delta_{\frac{5}{2}^+}(2000)$, which are the most prominent ones as stated in Ref. [12]. The coupling constants f_1 and f_2 can be calculated from the helicity amplitudes in PDG [19] or model predictions with Eq.(B3) of Ref. [12]. For $\gamma N \Delta$ coupling, we have $f_1 = 4.04$ and $f_2 = 3.87$. From the predicted helicity amplitudes in Ref. [20], one gets $f_1 = -1.25$ and $f_2 = 1.21$ for $\gamma p N^*(2080)$ coupling; $f_1 = 0.381$ and $f_2 = -0.256$ for $\gamma n N^*(2080)$ coupling; $f_1 = 0.39$ and $f_2 = -0.57$ for $\gamma N \Delta(1940)$ coupling, and $f_1 = -0.68$, $f_2 = -0.062$ for $\gamma N \Delta(2000)$ coupling. For $\Delta K \Sigma^*$ coupling, $h_1 = 2.0$ and $h_2 = 0$ are used from $h_1 = -f_{K\Delta\Sigma^*}/\sqrt{3}$ with $f_{K\Delta\Sigma^*} = -3.46$ [21]. For the resonances coupling to $K\Sigma^*$, the coupling constants h_1 and h_2 can be calculated from Eq.(B11)-(B18) of Ref. [12] from the model predicted amplitudes $G(l)$ [22]. In our concrete calculation, $h_1 = 0.24$ and $h_2 = -0.54$ for $N^*(2080)K\Sigma^*$ coupling, $h_1 = -0.68$ and $h_2 = 1.0$ for $\Delta(1940)K\Sigma^*$ coupling, and $h_1 = -1.1$ and $h_2 = 0.21$ for $\Delta(2000)K\Sigma^*$ coupling are taken.

The reaction $\gamma p \rightarrow K^+ \Sigma^{*0}$ contains the u-channel $\Lambda(1116)$ exchange. The effective Lagrangians are

$$\begin{aligned} \mathcal{L}_{\gamma \Lambda \Sigma^*} &= -\frac{ief_1}{2M_\Lambda} \bar{\Lambda} \gamma_\nu \gamma_5 F^{\mu\nu} \Sigma_\mu^* \\ &\quad - \frac{ef_2}{(2M_\Lambda)^2} \partial_\nu \bar{\Lambda} \gamma_5 F^{\mu\nu} \Sigma_\mu^* + H.c., \quad (11) \end{aligned}$$

$$\mathcal{L}_{KN\Lambda} = \frac{g_{KN\Lambda}}{M_N + M_\Lambda} \bar{N} \gamma^\mu \gamma_5 \Lambda \partial_\mu K + H.c., \quad (12)$$

where $f_1 = 4.52$, $f_2 = 5.63$ are obtained from decay width $\Gamma(\Sigma^* \rightarrow \Lambda\gamma)$ and model predicted helicity amplitudes; and $g_{KN\Lambda} = -13.24$ is estimated from flavor SU(3) symmetry relation as in Ref. [12].

For u-channel Σ^* exchange, the effective Lagrangian for $\gamma\Sigma^*\Sigma^*$ is

$$\mathcal{L}_{\gamma\Sigma^*\Sigma^*} = e\bar{\Sigma}_\mu^* A_\alpha \Gamma_{\gamma\Sigma^*}^{\alpha,\mu\nu} \Sigma_\nu^*, \quad (13)$$

with

$$A_\alpha \Gamma_{\gamma\Sigma^*}^{\alpha,\mu\nu} = Q_{\Sigma^*} A_\alpha (g^{\mu\nu} \gamma^\alpha - \frac{1}{2}(\gamma^\mu \gamma^\nu \gamma^\alpha + \gamma^\alpha \gamma^\mu \gamma^\nu)) - \frac{\kappa_{\Sigma^*}}{2M_N} \sigma^{\alpha\beta} \partial_\beta A_\alpha g^{\mu\nu}, \quad (14)$$

where Q_{Σ^*} denotes the electric charge of Σ^* in unit of e and κ_{Σ^*} denotes the anomalous magnetic moment of Σ^* ; $\kappa_{\Sigma^{*0}} = 0.36$ and $\kappa_{\Sigma^{*-}} = -2.43$ are taken from the quark model prediction [23].

For each vertex of these channels, a form factor is attached to describe the off-shell properties of the amplitudes. For t-channel K meson exchange, we adopt the form factor [12]

$$F_M = \frac{\Lambda_M^2 - m_K^2}{\Lambda_M^2 - q_t^2}, \quad (15)$$

where $q_t = k - q$ is the 4-momentum transfer in t-channel. For the s-channel and u-channel processes, we adopt the form factor

$$F_B(q_{ex}^2, M_{ex}) = \left(\frac{n\Lambda_B^4}{n\Lambda_B^4 + (q_{ex}^2 - M_{ex}^2)^2} \right)^n, \quad (16)$$

where the q_{ex} and M_{ex} are the 4-momentum and the mass of the exchanged hadron, respectively. For s-channel N and Δ exchange and the u-channel processes, we take $n = 1$ as in Ref. [12]; for s-channel resonances exchange, $n \rightarrow \infty$ is taken to obtain the Gaussian form for the form factors [12]

$$F_B(q_s^2, M_R)|_{n \rightarrow \infty} = \exp\left(-\frac{(q_s^2 - M_R^2)^2}{\Lambda_B^4}\right). \quad (17)$$

The cutoff parameters Λ_M and Λ_B were taken to be 0.83 and 1.0 GeV, respectively, in Refs. [9, 12], by fitting to the $\gamma p \rightarrow K^+\Sigma^{*0}$ data.

The contact term illustrated with Fig. 1(d) serves to keep the full amplitude gauge invariant. The contact currents for $K\Sigma^*$ photoproduction are related to the Lagrangian of Eq.(2). For the process $\gamma p \rightarrow K^+\Sigma^{*0}$, we adopt the contact current [12, 18]

$$M_c^{\mu\nu} = ie \frac{f_{KN\Sigma^*}}{m_K} (g^{\mu\nu} f_t - q^\mu C^\nu), \quad (18)$$

where C^ν is expressed as

$$C^\nu = -(2q - k)^\nu \frac{f_t - 1}{t - m_K^2} (1 - h(1 - f_s)) - (2p + k)^\nu \frac{f_s - 1}{s - M_N^2} (1 - h(1 - f_t)). \quad (19)$$

Here the Lorenz index μ and ν couple to that of Σ^* and the photon respectively; $f_t = F_M^2$ and $f_s = F_B^2(s, M_N)$ are form factors squared, and $t = q_t^2$ and $s = q_s^2$ are squared momentum transfer for t- and s-channel; h is a parameter to be fitted to experiments, and $h = 1$ is used in Ref.[12]. From this contact term, we can check that the total amplitude is gauge invariant. For the process $\gamma n \rightarrow K^+\Sigma^{*-}$, the contact current is [18]

$$M_c^{\mu\nu} = ie\sqrt{2} \frac{f_{KN\Sigma^*}}{m_K} (g^{\mu\nu} f_t - q^\mu C^\nu), \quad (20)$$

with

$$C^\nu = -(2q - k)^\nu \frac{f_t - 1}{t - m_K^2} (1 - h(1 - f_u)) + (2p' - k)^\nu \frac{f_u - 1}{u - M_{\Sigma^*}^2} (1 - h(1 - f_t)). \quad (21)$$

Where $f_u = F_B^2(u, M_{\Sigma^*})$ is form factor squared, and $u = q_u^2$ is squared momentum transfer for u-channel.

For the propagators, we use $1/(q_t^2 - m_K^2)$ for t-channel K meson exchange. For the propagator of a baryon with mass m and 4-momentum p , we use $\frac{p^\dagger + m}{p^2 - m^2}$ for spin-1/2 propagator;

$$\frac{p^\dagger + m}{p^2 - m^2} \left(-g^{\mu\nu} + \frac{\gamma^\mu \gamma^\nu}{3} + \frac{\gamma^\mu p^\nu - \gamma^\nu p^\mu}{3m} + \frac{2p^\mu p^\nu}{3m^2} \right) \quad (22)$$

for spin-3/2 propagator; and

$$\frac{p^\dagger + m}{p^2 - m^2} S_{\alpha\beta\mu\nu}(p, m) \quad (23)$$

for spin-5/2 propagator, where

$$S_{\alpha\beta\mu\nu}(p, m) = \frac{1}{2}(\bar{g}_{\alpha\mu}\bar{g}_{\beta\nu} + \bar{g}_{\alpha\nu}\bar{g}_{\beta\mu}) - \frac{1}{5}\bar{g}_{\alpha\beta}\bar{g}_{\mu\nu} - \frac{1}{10}(\bar{\gamma}_\alpha\bar{\gamma}_\mu\bar{g}_{\beta\nu} + \bar{\gamma}_\alpha\bar{\gamma}_\nu\bar{g}_{\beta\mu} + \bar{\gamma}_\beta\bar{\gamma}_\mu\bar{g}_{\alpha\nu} + \bar{\gamma}_\beta\bar{\gamma}_\nu\bar{g}_{\alpha\mu}), \quad (24)$$

with

$$\bar{g}_{\mu\nu} = g_{\mu\nu} - \frac{p_\mu p_\nu}{m^2}, \quad \bar{\gamma}_\mu = \gamma_\mu - \frac{p_\mu}{m^2} \not{p}. \quad (25)$$

For the s-channel resonances with sizeable width Γ , we replace the denominator $\frac{1}{p^2 - m^2}$ in the propagators by $\frac{1}{p^2 - m^2 + im\Gamma}$, and replace m in the rest of the propagators by $\sqrt{p^2}$.

B. $K\Sigma(\frac{1}{2}^-)$ photoproduction

Since five quark components for baryons may exist, there may be a $\Sigma(\frac{1}{2}^-)$ that has a large probability of five quark structure with mass near 1380 MeV as models predict [13, 16]. Both $\Sigma^*(\frac{3}{2}^+)$ and $\Sigma(\frac{1}{2}^-)$ decay strongly to

$\Lambda\pi$, which are detected by experiments. Thus we consider that $K\Sigma(\frac{1}{2}^-)$ photoproduction may also contribute to the measured cross sections. We constrain our study to processes with s and p wave hadronic vertices, since the contributions from higher waves are relatively suppressed. We also neglect the contributions from some resonances either for lack of information on the couplings or the couplings are small. Thus the main contributions to $K\Sigma(\frac{1}{2}^-)$ photoproduction are from the t-channel K meson exchange, the s-channel N exchange, the u-channel $\Sigma(\frac{1}{2}^-)$ exchange (and Λ exchange for $\gamma p \rightarrow K^+\Sigma^0(\frac{1}{2}^-)$) and the contact term. The Feynman diagrams are the same as Fig. 1. The effective Lagrangian for $KN\Sigma(\frac{1}{2}^-)$ coupling can be expressed as [21]

$$\mathcal{L}_{KN\Sigma} = -ig_{KN\Sigma}\overline{K}\overline{\Sigma}\cdot\tau N + \text{H.c.}, \quad (26)$$

where the coupling constant $g_{KN\Sigma}$ is to be fitted to experiments; The isospin structure is the same as Eq.(3). The effective Lagrangians for γKK and γNN are described in Eq.(1) and Eq.(4), respectively. For $\gamma\Sigma(\frac{1}{2}^-)\Sigma(\frac{1}{2}^-)$ vertex, the effective Lagrangian can be expressed as [21]

$$\mathcal{L}_{\gamma\Sigma\Sigma} = -e\overline{\Sigma}(\gamma^\mu A_\mu Q_\Sigma - \frac{\kappa_\Sigma}{2M_N}\sigma^{\mu\nu}\partial_\nu A_\mu)\Sigma, \quad (27)$$

where Q_Σ is the electric charge (in unite of e), and κ_Σ denotes the anomalous magnetic moment for $\Sigma(\frac{1}{2}^-)$, and we take the predicted values $\kappa_{\Sigma^0} = -0.43$ and $\kappa_{\Sigma^-} = -1.74$ from the diquark model [16]. For the $\gamma\Lambda\Sigma^0(\frac{1}{2}^-)$ coupling in the $\gamma p \rightarrow K^+\Sigma^0$ process, the effective Lagrangian is expressed as [21]

$$\mathcal{L}_{\gamma\Lambda\Sigma} = \frac{eg_{\gamma\Lambda\Sigma}}{4(M_\Lambda + M_\Sigma)}\overline{\Sigma}\gamma_5\sigma_{\mu\nu}\Lambda F^{\nu\mu} + \text{H.c.}, \quad (28)$$

where we take $g_{\gamma\Lambda\Sigma} = 1.16$. Note that although this coupling has some uncertainty, it is largely suppressed and has very small effect in this process.

For each vertex in the Feynman diagrams, a form factor is attached. Similar to the $K\Sigma^*(\frac{3}{2}^+)$ photoproduction processes, we adopt the form factor as in Eq.(15) for t-channel K meson exchange, and Eq.(16) for s-channel and u-channel processes.

The contact term for $K\Sigma(\frac{1}{2}^-)$ photoproduction is related to the Lagrangian of Eq.(26). Following Refs. [12, 18], we adopt the contact current

$$M_c^\nu = ieg_{KN\Sigma}C^\nu \quad (29)$$

for $\gamma p \rightarrow K^+\Sigma^0(\frac{1}{2}^-)$, where the Lorenz index ν couples to that of the photon, and C^ν is expressed as Eq.(19), where $h = 1$ is taken. For $\gamma n \rightarrow K^+\Sigma^-(\frac{1}{2}^-)$ process, we adopt the contact current:

$$M_c^\nu = ie\sqrt{2}g_{KN\Sigma}C^\nu, \quad (30)$$

where C^ν is expressed as Eq.(21), where $h = 1$ is taken. With these contact currents, one can check that the total amplitudes are gauge invariant.

Since previous evidence for the new $\Sigma(\frac{1}{2}^-)$ indicates its mass to be around $\Sigma^*(1385)$ [17], here we assume its mass be the same as $\Sigma^*(1385)$. The coupling constant $g_{KN\Sigma}$ and the relevant cut-off parameter Λ_M are unknown parameters, and will be tuned to fit the data.

III. RESULTS AND DISCUSSIONS

The effective Lagrangian methods employ hadronic fields as basic degrees of freedom for the interactions, which introduce many parameters such as the coupling constants and cutoff parameters. Many of the parameters are not well constrained, and approximations such as flavor SU(3) symmetry relation or model predictions are used. These may bring some uncertainty in the calculation. For example, in this paper, we consider 3 PDG resonances in s-channel as in Ref. [12]. Their masses, widths and coupling constants are not well constrained by experiments. Our choices of the parameters from the allowed range of PDG [19] and model calculations [20, 22] certainly have big uncertainties, similar as discussed in Ref. [24] for the study of $\gamma n \rightarrow K^+\Sigma^-$. However, for the cross sections and beam asymmetry of the reaction $\gamma n \rightarrow K^+\Sigma^*(1385) \rightarrow K^+\Lambda\pi^-$ at $E_\gamma = 1.5 - 2.4$ GeV reported by the LEPS collaboration [9], these 3 resonances mainly contribute to cross sections around $E_\gamma = 1.8$ GeV, and their contributions are small for $E_\gamma > 2.1$ GeV. Even without constraint from other sources, adjusting these parameters cannot reproduce the measured beam asymmetry qualitatively. We need to find other ingredients to describe the cross sections and beam asymmetry data simultaneously.

The measurement by the LEPS Collaboration is limited to forward angles with $\cos\theta_{c.m.} \geq 0.6$, where $\theta_{c.m.}$ is the forward angle of the produced K meson in the c.m. frame. The theoretical predictions by the original set of parameters ($h = 1$ for the contact term) [12] deviate from the LEPS results for the linear beam asymmetry [9], which can be interpreted as

$$A_{beam} = \frac{\sigma_\perp - \sigma_\parallel}{\sigma_\perp + \sigma_\parallel}, \quad (31)$$

where σ_\perp and σ_\parallel denote the cross sections for beam polarization vertical and parallel to the reaction plane, respectively.

In this work, we find two possible ingredients to explain the observed beam asymmetry. One is by including the possible contribution of $K\Sigma(\frac{1}{2}^-)$ photoproduction, and another is to assume a different h parameter for the γn reaction from the γp reaction. To incorporate the new ingredients to fit both cross sections and beam asymmetry, the minimum set of parameters to be adjusted from those used in Ref. [9, 12] are listed in Table I. For both schemes, the narrower widths for the three N^* and Δ^* resonances are used, but still within the PDG uncertainties [19]. The reached χ^2 of the two schemes are also

scheme	h	Λ_M	$\Gamma_{N^*(2080)}$	$\Gamma_{\Delta(1940)}$	$\Gamma_{\Delta(2000)}$	$g_{KN\Sigma}(\Lambda_M)$	χ^2
I	1.0 (fixed)	0.8 GeV	0.25 GeV	0.15 GeV	0.15 GeV	1.34 (1.6 GeV)	97
II	1.11					0 (fixed)	102
[9, 12] (PDG [19])	1.0 (fixed)	0.83	0.3 (0.12 ~ 0.63)	0.3 (0.10 ~ 0.78)	0.3 (0.07 ~ 0.52)	0 (fixed)	~ 180

TABLE I: Adjusted parameters for $\gamma n \rightarrow K^+\Sigma^{*-}$ with two schemes compared with original ones in Refs. [9, 12] and PDG range [19], and corresponding χ^2 for 39 data points in Figs. 3 & 4.

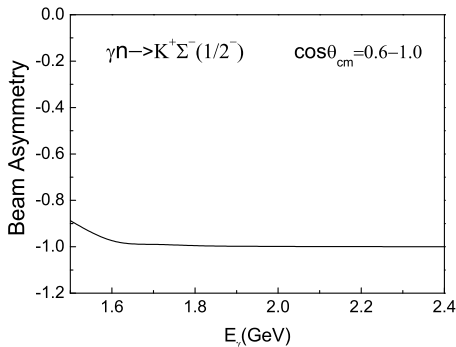


FIG. 2: Linear beam asymmetry for $\gamma + n \rightarrow K^+ + \Sigma^-(\frac{1}{2}^-)$ with $\cos\theta_{c.m.} = 0.6 - 1$.

listed. In scheme I, we keep $h = 1$ fixed for the contact term to be identical to the $\gamma p \rightarrow K^+\Sigma^{*0}$ process, and then include the contribution of $K\Sigma(\frac{1}{2}^-)$ photoproduction for the process. The coupling constant of $\Sigma(\frac{1}{2}^-)$ to KN and the corresponding cut-off parameter are tuned to describe the experimental data. In scheme II, we do not consider $\Sigma(\frac{1}{2}^-)$ production, and tune parameter h of the contact term to describe the data.

In Fig. 2 we show the result of the linear beam asymmetry for $\gamma n \rightarrow K^+\Sigma^-(\frac{1}{2}^-)$ with $\cos\theta_{c.m.} \geq 0.6$, *i.e.*, the cross sections in Eq. (31) are integrated results for $\cos\theta_{c.m.} = 0.6 - 1$. The process has a large negative beam asymmetry that approaches -1 . This result comes from the fact that $K^+\Sigma^-(\frac{1}{2}^-)$ is produced mainly from the t-channel kaon exchange process. For the t-channel kaon exchange process, the photon spin is necessary to be vertical to the reaction plane due to angular momentum conservation, and such photon corresponds to the beam (electromagnetic field) with polarization parallel to the reaction plane, *i.e.*, $\sigma_{\perp} = 0$. Thus the $K^+\Sigma^-(\frac{1}{2}^-)$ production contributes negatively to the beam asymmetry. If a portion of the detected $\Lambda\pi$ stems from $\Sigma(\frac{1}{2}^-)$, the measured beam asymmetry can be pulled to the negative side, and the observed negative beam asymmetry may be explained.

In Fig. 3, the differential cross sections for the process $\gamma n \rightarrow K^+\Sigma^{*-}$ with respect to $\cos\theta_{c.m.}$ are shown and compared with the LEPS data [9]. The solid lines are the results of scheme I, and the dashed lines are the results

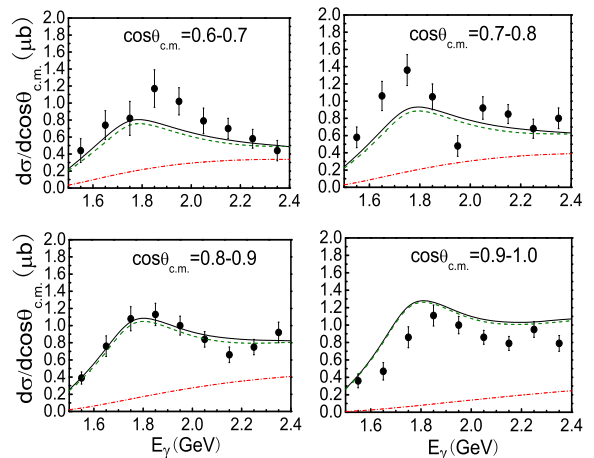


FIG. 3: Differential cross sections for $\gamma + n \rightarrow K^+ + \Sigma^{(*)-}$ with four $\cos\theta_{c.m.}$ intervals. Theoretical results with scheme I (solid curves) and scheme II (dashed curves) are compared with the LEPS data [9]. The dot-dashed curves demonstrate the contributions from $\Sigma(\frac{1}{2}^-)$ production in scheme I.

of scheme II. The contributions from $\Sigma(\frac{1}{2}^-)$ production in scheme I are also shown by the dash-dotted lines.

In Fig. 4 and Fig. 5, the results for the linear beam asymmetry and integrated cross sections of the reaction $\gamma n \rightarrow K^+\Sigma^{*-}$ are shown and compared with the LEPS data [9], respectively. The cross sections are intergrated results in phase space $\cos\theta_{c.m.} = 0.6 - 1.0$. The solid lines are the results of scheme I, *i.e.*, including both $\Sigma^*(\frac{3}{2}^+)$ production with $h = 1$ and the contribution from $\Sigma(\frac{1}{2}^-)$. The dashed lines are the results of scheme II, *i.e.*, for $\Sigma^*(\frac{3}{2}^+)$ production alone with $h = 1.11$. The dotted lines are the results with the $h = 1$ and without the contribution from $\Sigma(\frac{1}{2}^-)$. The contribution from $\Sigma(\frac{1}{2}^-)$ production to the cross section alone is shown by the dash-dotted line in Fig. 5.

From Fig.3-5, one can see that both schemes can well describe the LEPS data. For scheme I, since the $\Sigma(\frac{1}{2}^-)$ alone gives a large negative beam asymmetry approaching -1 as shown in Fig. 2, a portion of $\Sigma(\frac{1}{2}^-)$ in this process helps to explain the observed negative beam asymmetry. At the same time, we find that tuning the pa-

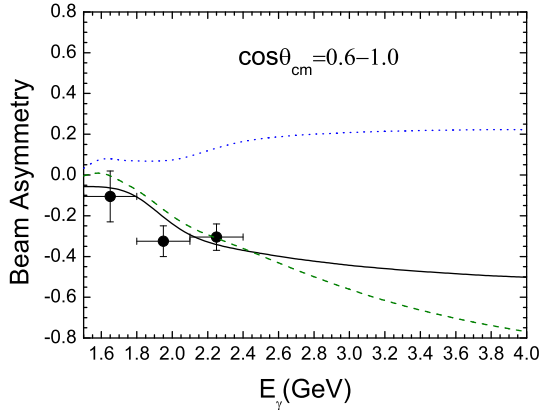


FIG. 4: The linear beam asymmetry for $\gamma + n \rightarrow K^+ + \Sigma^{(*)-}$ with $\cos\theta_{c.m.}$ integrated from 0.6 to 1.0. Results of scheme I (solid curve), and scheme II (dashed curve) are compared with the LEPS data [9]. The dotted curve demonstrate the result with $h = 1$ and without $\Sigma(\frac{1}{2}^-)$ contribution.

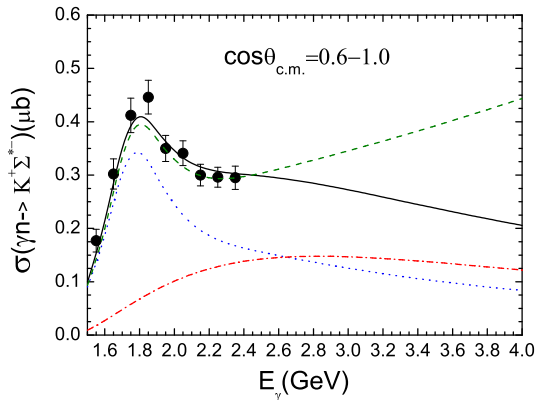


FIG. 5: Integrated cross sections for $\gamma + n \rightarrow K^+ + \Sigma^{(*)-}$ with $\cos\theta_{c.m.} = 0.6 - 1.0$ of scheme I (solid curve) and scheme II (dashed curve), compared with the LEPS data [9]. The dotted and dot-dashed curves demonstrate the contributions from $\Sigma^*(\frac{3}{2}^+)$ and $\Sigma(\frac{1}{2}^-)$, respectively, in the scheme I.

parameter h to a larger value as scheme II can also have such an effect. The χ^2 for the two schemes are 97 and 102, respectively, compared to the 39 experimental data points in Figs. 3 & 4. As a comparison, the corresponding previous theoretical prediction [9] without including the two new ingredients give a χ^2 value about 180.

From the comparison of the results with the LEPS data, one can not tell for sure which one of the two schemes is better. In fact, some other combinations of h and $g_{KN\Sigma}$, such as $h = 1.06$ combined with $g_{KN\Sigma} = 1.04$, may also describe the present data. However, one can

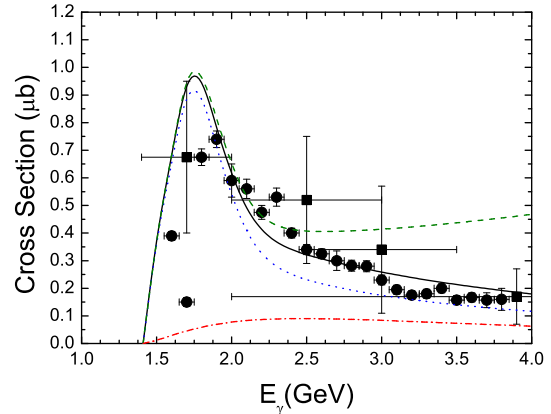


FIG. 6: Total cross sections for $\gamma + p \rightarrow K^+ + \Sigma^{(*)0}$ of scheme I (solid curve) and scheme II (dashed curve), compared with the CLAS preliminary data [2]. The dotted and dot-dashed curves demonstrate the contributions from $\Sigma^*(\frac{3}{2}^+)$ and $\Sigma(\frac{1}{2}^-)$, respectively, in the scheme I.

see from Fig. 5 that for higher incident energy, the two schemes give very distinctive predictions. Thus the schemes and mechanisms can be distinguished when data on reaction $\gamma n \rightarrow K^+ \Sigma^{*-}$ at higher incident energies are available.

The above results show that while the original theoretical prediction with $\Sigma^*(\frac{3}{2}^+)$ production alone with $h = 1$ fails to reproduce the data for $\gamma n \rightarrow K^+ \Sigma^{*-}$ [9, 12], the data can be well reproduced either by increasing h to 1.11 or by including an additional $\Sigma(\frac{1}{2}^-)$ resonance around 1380 MeV. Since the parameters for the original theoretical prediction come from the fits to the data on the $\gamma p \rightarrow K^+ \Sigma^{*0}$ process, we need to check how the new sets of parameters fit to the $\gamma p \rightarrow K^+ \Sigma^{*0}$ data. The results are shown in Fig. 6 for the total cross sections of the reaction $\gamma p \rightarrow K^+ \Sigma^{*0}$ with the above sets of parameters, comparing with the CLAS data [2]. Again, the solid line is the result for $\Sigma^*(\frac{3}{2}^+)$ production with $h = 1$ combined with the contribution from $\Sigma(\frac{1}{2}^-)$ with $g_{KN\Sigma} = 1.34$; the dotted line and the dashed line are the results for $\Sigma^*(\frac{3}{2}^+)$ production alone with $h = 1$ and $h = 1.11$, respectively. The $\Sigma(\frac{1}{2}^-)$ contribution is also shown by the dash-dotted line with $g_{KN\Sigma} = 1.34$. From Fig. 6 one sees that the combined result of $\Sigma^*(\frac{3}{2}^+)$ production with $h = 1$ and the $\Sigma(\frac{1}{2}^-)$ production (scheme I, solid line) can be compatible with the CLAS data on the whole, while the results with $h = 1.11$ (dashed line) deviate from the data for larger incident energy.

Our results show that the combined results of $\Sigma^*(\frac{3}{2}^+)$ and $\Sigma(\frac{1}{2}^-)$ production (solid line) can be compatible with both the $\gamma n \rightarrow K^+ \Sigma^{*-}$ reaction data and the $\gamma p \rightarrow K^+ \Sigma^{*0}$ reaction data with the same set of parameters

(scheme I). Without the $\Sigma(\frac{1}{2}^-)$ contribution, different parameter h need to be used for $\gamma n \rightarrow K^+\Sigma^{*-}$ and $\gamma p \rightarrow K^+\Sigma^{*0}$ processes.

The properties and couplings for $\Sigma(\frac{1}{2}^-)$, the contact term, and the s-channel resonances still have some uncertainties and need further investigation. More data of broader energy range on these processes will be helpful to clarify the roles of the contact term and the $\Sigma(\frac{1}{2}^-)$ resonance.

IV. SUMMARY

In summary, we study the process of $K\Sigma^*(1385)$ photoproduction from the nucleons in the framework of the effective Lagrangian method. From recent studies, there is possibly a Σ state with $J^P = \frac{1}{2}^-$ near 1380 MeV. We consider the case that $\Sigma(\frac{1}{2}^-)$ may contribute to the observables of $K\Sigma^*(1385)$ photoproduction in experiments. Our results show that the $\Sigma(\frac{1}{2}^-)$ production can give large negative contribution to beam asymmetry, which helps to explain the large negative linear beam asymme-

try observed by the LEPS experiment. With a portion of $\Sigma(\frac{1}{2}^-)$, the same set of parameters can reproduce both the data of $\gamma n \rightarrow K^+\Sigma^{*-}$ from the LEPS experiment and the data of $\gamma p \rightarrow K^+\Sigma^{*0}$ from the CLAS experiment. On the other hand, without including $\Sigma(\frac{1}{2}^-)$, the present data on $\gamma n \rightarrow K^+\Sigma^{*-}$ can be described by tuning a parameter h in the contact term, which means different choices of parameter h in the contact term for γn and γp reactions are needed. To distinguish the roles of $\Sigma(\frac{1}{2}^-)$ and the contact term, different predictions of the two schemes are presented for future experimental study.

Acknowledgments

We thank Kanzo Nakayama and Yongseok Oh for the helpful discussions. This project is supported by the National Natural Science Foundation of China under Grant 10905059, 10875133, 10821063, and by China Postdoctoral Science Foundation and the Ministry of Science and Technology of China (2009CB825200).

-
- [1] R. Bradford *et al.* (CLAS Collaboration), Phys. Rev. C **73**, 035202 (2006).
 - [2] L. Guo and D.P. Weygand (CLAS Collaboration), in *Proceedings of the International Workshop on the Physics of Excited Baryons (NSTAR05)*, edited by S. Capstick, V. Crede, and P. Eugenio (World Scientific, Singapore, 2006, pp. 306-309).
 - [3] I. Hleiqawi *et al.* (CLAS Collaboration), Phys. Rev. C **75**, 042201(R) (2007); Phys. Rev. C **76**, 039905(E) (2007).
 - [4] M. Nanova *et al.* (CBELSA/TAPS Collaboration), Eur. Phys. J. A **35**, 333 (2008).
 - [5] M.Q. Tran *et al.* (SAPHIR Collaboration), Phys. Lett. B **445**, 20 (1998).
 - [6] R.G.T. Zegers *et al.*, Phys. Rev. Lett. **91**, 092001 (2003).
 - [7] M. Sumihama *et al.* (LEPS Collaboration), Phys. Rev. C **73**, 035214 (2006).
 - [8] M. Niiyama *et al.*, Phys. Rev. C **78**, 035202 (2008).
 - [9] K. Hicks *et al.* (LEPS Collaboration), Phys. Rev. Lett. **102**, 012501 (2009).
 - [10] M.F.M. Lutz and Soyeur, Nucl. Phys. A **748**, 499 (2005).
 - [11] M.Döring, E. Oset, and M. Strattman, Phys. Lett. B **639**, 59 (2006); Phys. Rev. C **73**, 045209 (2006).
 - [12] Y. Oh, C.M. Ko, and K. Nakayama, Phys. Rev. C **77**, 045204 (2008).
 - [13] C. Helminen and D.O. Riska, Nucl. Phys. A **699**, 624 (2002).
 - [14] B.S. Zou, Eur. Phys. J. A **35**, 325 (2008); Int. J. Mod. Phys. A **21**, 5552 (2006).
 - [15] R. Jaffe and F. Wilczek, Phys. Rev. Lett. **91**, 232003 (2003).
 - [16] A. Zhang *et al.*, High Energy Phys. Nucl. Phys. **29**, 250 (2005).
 - [17] J.J. Wu, S. Dulat, and B.S. Zou, Phys. Rev. D **80**, 017503 (2009); arXiv:0909.1380 [hep-ph].
 - [18] H. Haberzettl, K. Nakayama, and S. Krewald, Phys. Rev. C **74**, 045202 (2006).
 - [19] Particle Data Group, C. Amsler *et al.*, Phys. Lett. B **667**, 1 (2008).
 - [20] S. Capstick, Phys. Rev. D **46**, 2864 (1992).
 - [21] Y. Oh, K. Nakayama, and T.-S.H. Lee, Phys. Rep. **423**, 49 (2006).
 - [22] S. Capstick and W. Roberts, Phys. Rev. D **58**, 074001 (1998).
 - [23] D. B. Lichtenberg, Phys. Rev. D **15**, 345 (1977).
 - [24] P. Vancraeyveld *et al.*, Phys. Lett. B **681**, 428 (2009).